ACADÉMIE DES SCIENCES
INSTITUT DE FRANCE

Comptes Rendus. Géoscience — Sciences de la Planète
Supplementary material to the article available at:
https://doi.org/10.5802/crgeos.243

Research article

Potential and limitations of noise-based surface-wave tomography for numerical site effect estimation: a case study in the French Rhône valley

François Lavoué [*,a,b], Bérénice Froment [a], Céline Gélis [a], Pierre Boué [b], Emmanuel Chaljub [b], Laurent Stehly [b], Sophie Beauprêtre [c], Florent De Martin [d], Loïc Gisselbrecht [a,b], Marco Pilz [e], Denis Moiriat [a] and Edward Marc Cushing [a]

[a] Institut de Radioprotection et Sûreté Nucléaire (IRSN), PSE-ENV, SCAN, BERSSIN/BEHRIG, Fontenay-aux-Roses, France

[b] Univ. Grenoble Alpes, Univ. Savoie Mont Blanc, CNRS, IRD, UGE, ISTerre, Grenoble, France

[c] Sisprobe/EGIS, 3 rue du Dr Schweitzer, 38180 Seyssins, France

[d] BRGM (French Geological Survey), Risks and Prevention Division, Orléans, France

[e] GFZ, German Research Center for Geosciences, Potsdam, Germany

E-mail: francois.lavoue@univ-grenoble-alpes.fr (F. Lavoué)

Description of the supplementary material

This supplementary material contains:

1. A movie of the simulated wavefield on the free surface of the numerical model.
2. A catalog of amplification curves computed using the Standard Spectral Ratio technique (SSR, Borcherdt, 1970) for each station of the DARE broadband network.

1. Movie of the simulated wavefield

File S1 contains a movie showing the propagation of seismic waves on the free surface of the simulation domain (excluding 15-km-wide margins). The N–S component of particle velocity (v_y) is shown, for a vertically-incident SH excitation polarized in the N–S direction. Please note that the unrealistic amplitudes indicated on the color bar (±7 m/s) are purely conventional, and due to the injection of a 1-m maximum displacement at 5 km depth.

Annotations: Blue triangles correspond to broadband stations. The dotted line delineates the part of the domain that is constrained by the tomography. The solid black line corresponds to the 375-m-depth iso-contour of the interface between sediments and bedrock in the tomographic model. The location of the Tricastin Nuclear Site (TNS) is also indicated.

2. Catalog of amplification curves

One of the two DARE campaigns consisted of deploying about 50 broadband stations over the study area for more than eight months and targeted the recording of seismicity (including teleseismic events, regional, and local seismicity, [Pilz et al., 2021]).

The sites were instrumented with DATA-Cube3 and three-component Trillium compact 120 s. This dataset was presented in detail in Froment et al. [2022].

* Corresponding author.

Seismicity data recorded by this network is used in the present paper to compare our numerical estimations of seismic amplification with observations.

File S2 shows the SSR curves as a function of frequency for each station obtained from the processing of this seismicity data as follows:

- Pre-selection of earthquakes using recordings at station A04, based on ISC (International Seismological Centre) catalogue, magnitude relative to the epicentral distance, signal-to-noise ratio (SNR) and visual inspection. The derived catalog consists in 424 events [Froment et al., 2022];
- Station A04 located on Urgonian limestones outside the Messinian canyon in a quiet area (see Map S1 below) is used as reference station for SSR computation (amplitude of HVSR ≃ 1).
- Data processing: for each earthquake and each station,
  - Signal and noise windows are selected at the station of interest and at the reference (A04).
  - The frequency band for which SNR is ≥3 is determined (the frequency band is considered usable if its width is larger than 1 Hz).
  - The amplification is computed using the SSR technique [Borcherdt, 1970].
- Following these quite restrictive criteria, 27 earthquakes were selected for the SSR calculation (see Table S1 and Map S2 below). SSR curves obtained for each event and each component are gathered in **top figures of the catalog**.
- For each station, the SSR averaged over the different earthquakes and its standard deviation are computed. This mean SSR (solid line), plus/minus one standard deviation (dashed lines), are shown in **bottom figures of the catalog**.

There is no SSR computation for stations A05, E02, E06, and F00 because no earthquake signal fulfills the above criteria for these stations.

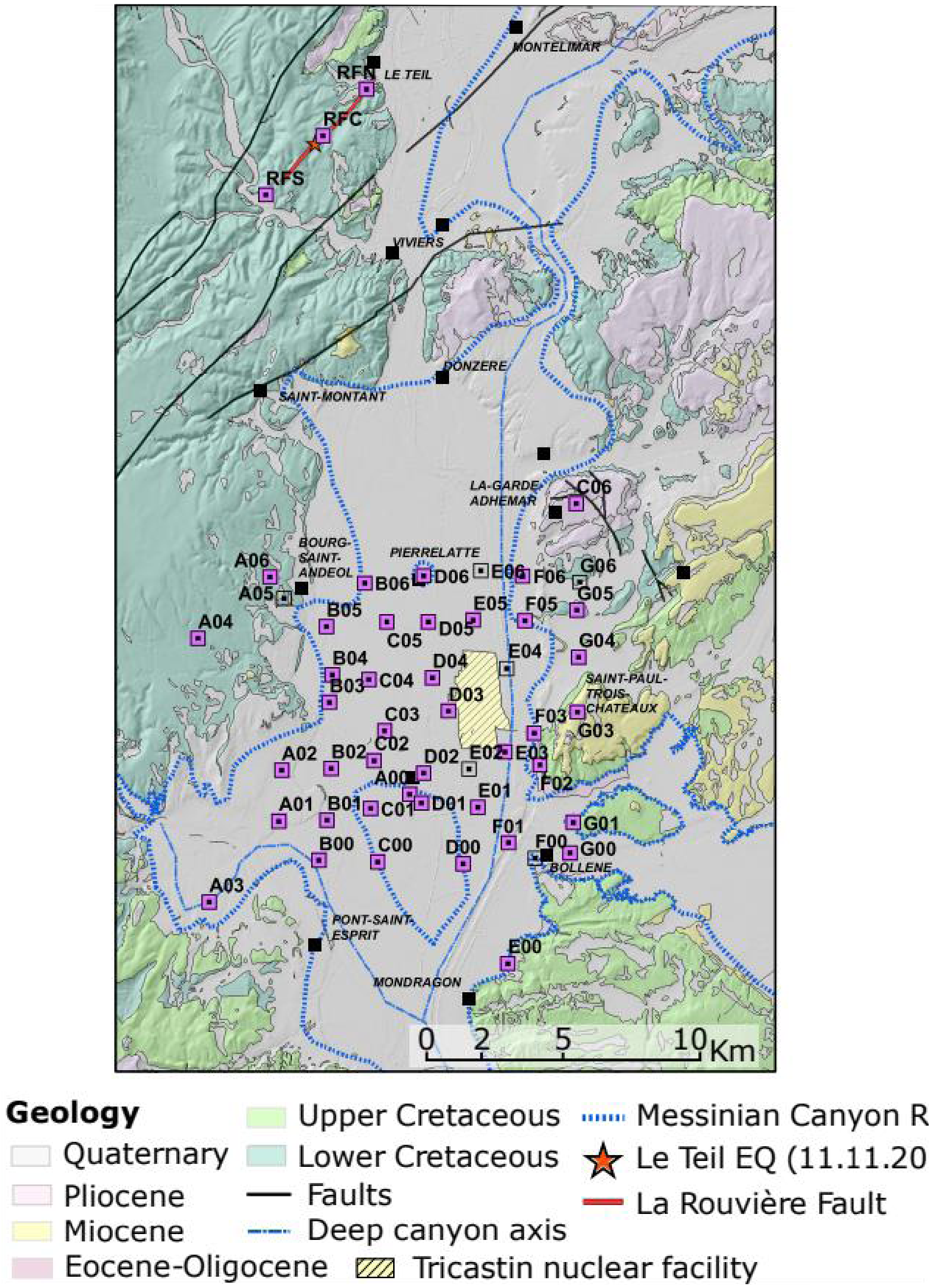

Supplementary Map S1. Location of the broadband stations deployed during the DARE project [from Froment et al., 2022].

Supplementary Table S1. Selected earthquakes for the SSR calculation

Earthquake name	Longitude	Latitude	Magnitude	Epicentral distance (km)	Backazimuth (deg)
Alaska	−159.7500	54.7100	7.5	8911	274
Algeria	6.7600	36.6500	5.3	876	166
Algeria2	5.2400	36.9300	6.0	830	176
Aoste	7.4700	45.9600	3.9	276	60
Balkans3	16.2500	45.4000	5.1	912	85
Berne	7.4200	46.8800	3.5	347	47
Croatia	16.2187	45.4002	6.4	909	85
Dodecanese	26.8310	37.8442	5.6	1980	106
Genes	9.8800	44.6000	3.9	407	87
Greece2	22.1900	39.7400	6.2	1526	105
Haguenau	7.8000	48.7000	3.8	537	35
Narbonne	3.1500	43.0800	3.8	194	231
NordItaly	9.0673	45.4277	3.8	359	76
Pamplune3	−1.4700	42.8300	3.5	531	256
Pamplune6	−1.5300	42.9300	3.7	532	257
Poitiers	0.1000	46.6000	3.7	441	295
Pyrenees	−1.5799	42.9021	5.9	537	257
Pyrenees2	−1.4691	42.8418	3.8	531	256
Pyrenees3	−1.6740	42.9950	4.6	541	258
SeoUrgel	1.6200	42.3200	3.8	342	237
SeoUrgel2	1.6200	42.3300	3.6	342	237
Strasbourg	7.7000	48.7000	3.8	531	34
Stuttgart	9.0200	48.3200	3.9	547	47
Stuttgart2	9.0500	48.3500	4.1	551	47
Switzerland	9.1308	46.8727	4.2	439	60
Vaduz	9.1200	46.9000	3.9	440	60
Vaduz2	9.1300	46.9200	3.7	442	60

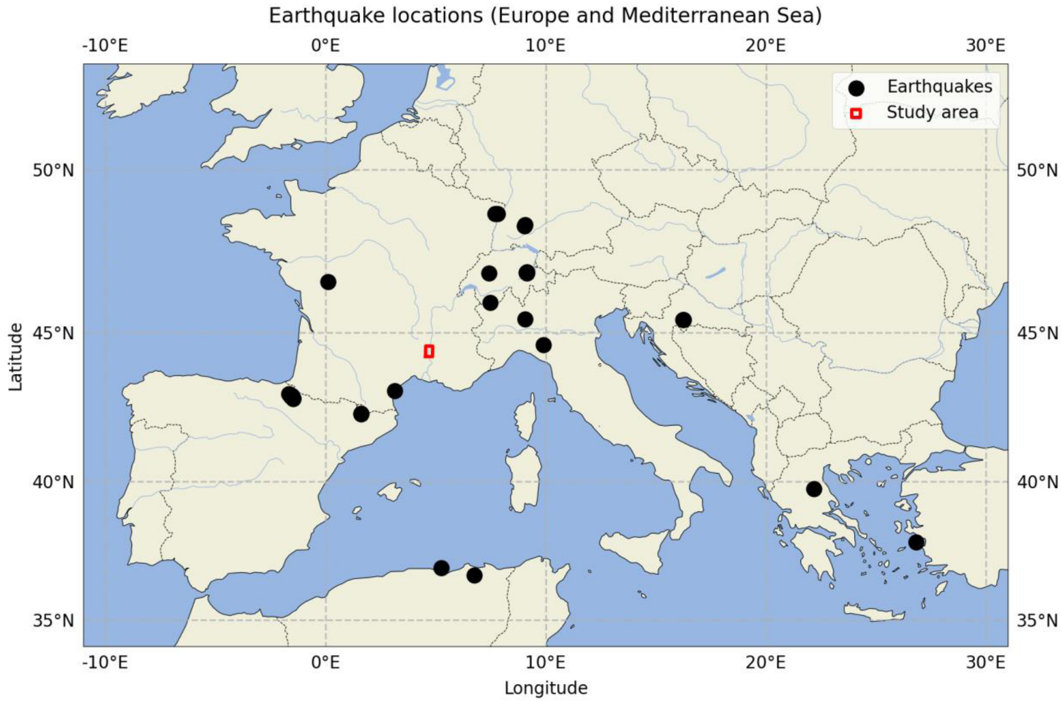

Supplementary Map S2. Location of selected earthquakes in the Euro-Mediterranean zone (only the Alaska earthquake from Table S1 is out of this area).

References

Borcherdt, R. D. (1970). Effects of local geology on ground motion near San Francisco Bay. *Bull. Seismol. Soc. Am.*, 60(1), 29–61.

Froment, B., Olivar-Castaño, A., Ohrnberger, M., Gisselbrecht, L., Hannemann, K., Cushing, E. M., Boué, P., Gélis, C., Haendel, A., Pilz, M., Hillmann, L., Barbaux, O., Beauprêtre, S., Bouzat, G., Chaljub, E., Cotton, F., Lavoué, F., Stehly, L., Zhu, C., Magnin, O., Métral, L., Mordret, A., Richet, Y., and Tourette, A. (2022). Complementary dense datasets acquired in a low-to-moderate seismicity area for characterizing site effects: application in the French Rhône valley. *Seismol. Res. Lett.*, 94(1), 531–547.

Pilz, M., Cotton, F., Ohrnberger, M., and Froment, B. (2021). DARE: Dense ARray for seismic site effect estimation. GFZ Data Services. Seismic Network.